Chinese Journal of Electronics
Vol.32, No.5, Sept. 2023

A Novel Blind Detection Algorithm Based on Spectrum Sharing and Coexistence for Machine-to-Machine Communication

ZHANG Yun[1,2], ZHOU Jing[1,2], LIU Rong[1,2], YU Shujuan[1,2], and LI Binrui[1,2]

(1. *College of Electronic and Optical Engineering, Nanjing University of Posts and Telecommunications, Nanjing 210023, China*)

(2. *College of Flexible Electronics (Future Technology), Nanjing University of Posts and Telecommunications, Nanjing 210023, China*)

Abstract — This paper proposes a new scheme that allows decentralized machine-to-machine (M2M) communication to share spectrum with conventional user communication in an orthogonal frequency division multiplexing system. This scheme can effectively separate and recover mixed signals at the receiving end. It mainly uses the signal space cancellation-complex system Hopfield neural network (SSC-CSHNN) blind detection algorithm to reconstruct the complementary projection operator and the blind detection performance function to restore the M2M communication signals. In order to further improve the anti-interference performance of the system and accelerate the convergence of the algorithm, the double sigmoid idea is introduced, and the signal space cancellation-double sigmoid complex system Hopfield neural network (SSC-DSCSHNN) blind detection algorithm is proposed. The proposed blind detection algorithm improves the anti-interference ability and the convergence speed and prevents the Hopfield neural network from falling into the local optimal solution based on the successful separation and recovery of mixed signals. Compared with existing methods, the blind detection algorithm used in this paper can directly detect the transmitted signal without identifying the channel.

Key words — Machine-to-machine communication, 5G, Spectrum sharing, Signal space cancellation, Complex Hopfield neural network, Blind detection.

I. Introduction

Due to the widespread application of machine-to-machine (M2M) communications in Internet of things, sensor networks, smart meters, and intelligent health, people are increasingly interested in M2M communications [1]. In the future, terminals used for human-to-human (H2H) communications may only account for 1/3 of the entire market, while the remaining will be used for M2M communication, which will inevitably lead to the lack of wireless spectrum resources [2]. Most M2M communications have some common properties, such as a large number of devices, extremely low data rates, and highly sporadic transmissions, while cellular systems based on local area networks are basically designed for H2H communications. H2H communications have different characteristics compared with M2M communications, which makes cellular systems unsuitable for M2M applications and services [3], [4]. This problem contradicts the increasingly scarce spectrum resources and becomes a bottleneck restricting the development of M2M communications.

Many researchers have proposed solutions to support M2M communication spectrum sharing and coexistence. To improve the M2M support scheme of global system for mobile communications (GSM), the scheme supporting M2M communication in the Long-Term Evolution Standard (LTE) architecture is proposed in [5]. The M2M communication scheduling scheme based on the LTE cellular system is proposed in [6], which uses the orthogonal frequency division multiple access (OFDMA) technology to share specific frequency and time resources in the user's system architecture. To support future M2M communication in cellular systems, a random access scheme for fixed-position M2M communication in OFDMA-based cellular systems is pro-

Manuscript Received July 24, 2021; Accepted Feb. 14, 2023. This work was supported by the National Natural Science Foundation of China (61977039).
 DOI:10.23919/cje.2021.00.244

posed in [7].

However, how to efficiently separate and recover transmission signals is a major difficulty for M2M spectrum sharing and coexistence systems. A spectrum sharing scheme based on compressed sensing for M2M Communication is proposed in [8], which utilizes the redundancy of transmission signals to separate mixture and compression sensing techniques are then used to detect jointly all the transmitted signals from the mixture. In orthogonal frequency division multiplexing (OFDM) system, reference [9] solves the problem of random access channel (RACH) congestion by allowing large-scale M2M devices and H2H communications to share the entire spectrum of the system assuming. However, the above schemes are all implemented on the premise of using the training sequence to estimate the transmission channel in advance. We all know that frequent use of training sequences increases the channel overhead and does not meet the time-varying and unknown characteristics of the actual transmission channel.

The blind detection technology can detect the transmitted signal only relying on the signal obtained by the receiving end without using a training sequence. A blind constellation detection method that meets the requirements of the fifth-generation (5G) system for higher spectral efficiency is proposed in [10]. A new type of autonomous unauthorized high-load non-orthogonal multiple access (NOMA) blind multi-user detection framework is described in [11], which is designed to meet the requirements of 5G large-scale machine-like communications. For sparse quadrature amplitude modulation (QAM) signals, a blind detection algorithm based on complex discrete is proposed in [12]. For the OFDM signal receiver, a continuous Hopfield neural network is designed in [13], which can significantly improve the bit error rate (BER) performance. A scheme that uses the redundancy in the transmitted signals to separate mixture under compressed sensing technology and uses the complex system Hopfield neural network (CSHNN) blind detection algorithm to recover the conventional user signals is proposed in [14]. However, the plan does not further analyze the performance of M2M communications.

In this paper, we consider the problem where a large number of sporadic M2M devices share the same unknown channel with a conventional communication user such as a cellular user. We will show that the signal space cancellation (SSC) can be exploited to separate the mixtures and the CSHNN blind detection algorithm can be used to detect the mixtures. We have made the following contributions.

1) We introduced the SSC and proposed the improved SSC-complex system Hopfield neural network (SSC-CSHNN) by selecting the appropriate improved activation function.

2) In order to further improve the anti-interference performance of the system and accelerate the convergence of the algorithm, the double sigmoid idea is introduced, and the SSC-double sigmoid CSHNN (SSC-DSC-SHNN) blind detection algorithm is proposed.

3) We selected the combination of activation functions with better anti-noise performance and convergence speed by comparing the blind detection algorithms formed by different double sigmoid activation functions.

The remainder of this paper is organized as follows. In Section II, we give the system model and the transmission scheme. In Section III, we detect conventional user signals; In Section IV, we develop a new blind detection algorithm to restore M2M communication signals, and we develop an algorithm to improve performance. Simulations are presented in Section V, and conclusions are given in Section VI.

II. System Model

In this paper, we consider a system in which M M2M devices transmit in a dispersed state and share the same over-sampling channel with the persistently conventional user. This makes M2M applications have low duty cycles and low data rates. We assume the M2M devices and conventional users use OFDM modulation to transmit signals which contain N OFDM symbols in each OFDM block, then the $N \times 1$ symbol vector $\boldsymbol{s}_i(m) = [s_i(m), \ldots, s_i(m+N-1)]^{\mathrm{T}}$ can be constructed, where $i = 0, \ldots, M$. The schematic diagram of the blind detection algorithm based on the spectrum sharing and coexistence for M2M communications is shown in Fig.1.

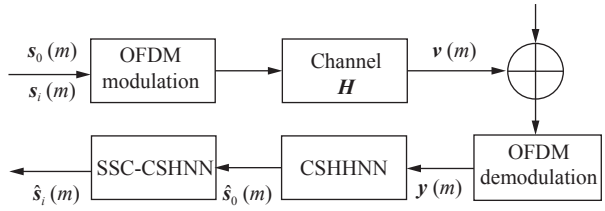

Fig. 1. Schematic of the blind detection algorithm based on spectrum sharing and coexistence for M2M communications.

In Fig.1, $\boldsymbol{s}_0(m)$ and $\hat{\boldsymbol{s}}_0(m)$ represent the conventional user's transmitted signal and its estimated signal respectively. $\boldsymbol{s}_i(m)$ and $\hat{\boldsymbol{s}}_i(m)$ represent the M2M device's transmitted signal and its estimated signal respectively. $\boldsymbol{H}$ is the over-sampling channel; $\boldsymbol{v}(m)$ consists of additive white Gaussian noise with zero mean and variance σ_v^2.

After OFDM modulation and demodulation, blind

detection system for M2M communication spectrum sharing receives the signal vector $\boldsymbol{y}(m)=[y(m),\ldots,y(m+N-1)]^{\mathrm{T}}$, and the receiving equation is

$$(\boldsymbol{y}(m))_{q\times 1}=\sum_{j=0}^{P}\sum_{i=0}^{M}(\boldsymbol{h}_j)_{q\times 1}\,s_i\,(m-j)+(\boldsymbol{v}(m))_{q\times 1} \tag{1}$$

where q is the channel oversampling factor, and P is the order of the channel, M is the number of M2M devices; $(\boldsymbol{h}_j)_{q\times 1}$ is the impulse response of the channel.

In the case of ignoring the noise $\boldsymbol{v}(m)$, the above receiver (1) can be written as

$$\boldsymbol{Y}=\boldsymbol{S}\boldsymbol{\Gamma}^{\mathrm{T}} \tag{2}$$

where $\boldsymbol{S}=[\boldsymbol{s}_{L+P}(m),\ldots,\boldsymbol{s}_{L+P}(m+N-1)]^{\mathrm{T}}=[\boldsymbol{s}_N(k),\ldots,\boldsymbol{s}_N(m-P-L)]_{N\times(L+P+1)M}$ is the conventional user transmit signal matrix; $(\boldsymbol{Y})_{N\times(L+1)q}=[\boldsymbol{y}_L(m),\ldots,\boldsymbol{y}_L\,(m+N-1)]^{\mathrm{T}}$ is the receive matrix of the conventional user; $(\boldsymbol{\Gamma})_{(L+1)q\times M(L+P+1)}$ is block Toeplitz matrix which consists of the channel impulse response $[\boldsymbol{h}_0,\ldots,\boldsymbol{h}_P]_{q\times(P+1)}$.

$$\boldsymbol{\Gamma}=\begin{bmatrix} h_0 & h_1 & \cdots & h_P & 0 & \cdots & 0\\ 0 & h_0 & \cdots & \cdots & h_P & \ddots & \vdots\\ \vdots & \ddots & \ddots & \ddots & \ddots & \ddots & 0\\ 0 & \cdots & 0 & h_0 & \cdots & \cdots & h_P \end{bmatrix}_{(L+1)q\times M(P+L+1)}$$

When $i=0$, the formula

$$\sum_{j=0}^{P}(\boldsymbol{h}_j)_{q\times 1}\,s_0\,(m-j) \tag{3}$$

is the matrix obtained by the conventional user transmitted signal $\boldsymbol{s}_0(m)$ after channel; when $i=1,\ldots,M$, the formula

$$\sum_{j=0}^{P}\sum_{i=1}^{M}(\boldsymbol{h}_j)_{q\times 1}\,s_i\,(m-j) \tag{4}$$

is the matrix obtained by the M2M devices transmitted signals $\boldsymbol{s}_i(m)$ after channel.

When an L order filter is used to equalize the received signal $\boldsymbol{y}(m)$, the received signal vector of length $(L+1)q$ can be expressed as

$$\begin{aligned}&(\boldsymbol{y}_L(m))_{1\times(L+1)q}\\&\quad=(\boldsymbol{s}_{L+P}(m))_{1\times(P+L+1)M}\cdot\boldsymbol{\Gamma}_L\,(\boldsymbol{h})+\boldsymbol{v}_L(m)\end{aligned} \tag{5}$$

where L is the parameter of equalizer; the output of the equalizer $(\boldsymbol{g}_j)_{(L+1)q\times 1}$ on the received signal is

$$\begin{aligned}s_{Nj}&=\boldsymbol{y}_L(m)\cdot g_j\\&=((\boldsymbol{s}_{L+P}(m))\,\boldsymbol{\Gamma}_L\,(\boldsymbol{h})+\boldsymbol{v}_L(m))\cdot g_j\end{aligned} \tag{6}$$

In this paper, conventional user communication signals and M2M communication signals are not related to noise.

III. Receiver and Conventional User Signal Detection

1. Blind detection performance function of receiver signal

The effect of the equalizer $\boldsymbol{g}$ on the $N\times(L+1)q$ dimensional received data array $\boldsymbol{Y}_N$ which is composed of N consecutive $\boldsymbol{y}_L(m)$ can be expressed as

$$\boldsymbol{Y}_N\cdot\boldsymbol{g}=\left[\boldsymbol{S}_N\cdot\boldsymbol{\Gamma}_L^{\mathrm{T}}+\boldsymbol{V}\right]\cdot\boldsymbol{g}=\hat{\boldsymbol{S}}_N+\boldsymbol{E}_0 \tag{7}$$

We define

$$\boldsymbol{E}_0=\boldsymbol{Y}_N\cdot\boldsymbol{g}-\hat{\boldsymbol{S}}_N=\boldsymbol{V}\cdot\boldsymbol{g} \tag{8}$$

where

$$\begin{aligned}\boldsymbol{Y}_N&=\left\{[y_L(m)\,,y_L(m+1),\ldots,y_L(m+N)]^{\mathrm{T}}\right\}_{N\times(L+1)q}\\\boldsymbol{S}_N&=\left[\boldsymbol{S}_{N0},\boldsymbol{S}_{N1},\ldots,\boldsymbol{S}_{Nj},\ldots,\boldsymbol{S}_{N(P+L)}\right]_{N\times(P+L+1)M}\\\boldsymbol{S}_{Nj}&=\{[\boldsymbol{s}_M(n-j),\boldsymbol{s}_M(n-j+1),\ldots,\\&\qquad\boldsymbol{s}_M(n-j+N)]^{\mathrm{T}}\}_{N\times M},\ \ j=0,\ldots,(P+L)\\\boldsymbol{E}_0&=\{[\boldsymbol{\varepsilon}_{01},\boldsymbol{\varepsilon}_{02},\ldots,\boldsymbol{\varepsilon}_{0M}]\}_{N\times M}\end{aligned}$$

In (7), $\boldsymbol{Y}_N$ is the only known quantity. For such blind problems where $\hat{\boldsymbol{S}}_N$ and $\boldsymbol{g}$ are unknown, the blind detection algorithm can be used to convert the blind detection problem into a quadratic optimization problem, and the solution target can be concentrated on $\hat{\boldsymbol{S}}_N$ with the help of a complementary space projection operator. Under the constraints of the transmitted signal character set $\boldsymbol{S}_N\in\{\pm1\ \pm i\}$, let $\boldsymbol{Q}=\boldsymbol{U}_n\cdot\boldsymbol{U}_n^{\mathrm{T}}$ be the complementary projection operator of $\hat{\boldsymbol{S}}_N$, then the zeroing residual equation is

$$(\boldsymbol{E})_{N\times M}=\boldsymbol{Q}\boldsymbol{\eta}_N=\boldsymbol{Q}\left(\boldsymbol{X}_N\boldsymbol{g}-\hat{\boldsymbol{S}}_N\right)=-\boldsymbol{Q}\hat{\boldsymbol{S}}_N \tag{9}$$

where $\boldsymbol{E}=[\boldsymbol{\varepsilon}_1,\ldots,\boldsymbol{\varepsilon}_M]_{N\times M}$, when the noise matrix $\boldsymbol{V}=\boldsymbol{0}$, the spatial residual is $\boldsymbol{E}=\boldsymbol{0}$.

The corresponding least squares performance function is

$$J\,(\boldsymbol{S}_N)=\boldsymbol{E}^{\mathrm{T}}\boldsymbol{E}=\boldsymbol{s}_N^{\mathrm{T}}\boldsymbol{Q}\boldsymbol{s}_N \tag{10}$$

Therefore, the estimated transmission sequence $\hat{\boldsymbol{S}}_N$ can be obtained by the direct blind detection algorithm of the following quadratic programming problem:

$$\hat{\boldsymbol{S}}_N = \arg \min_{\forall \boldsymbol{s}_N \in \{\pm 1 \pm i\}^N} J\left(\boldsymbol{S}_N\right) = \arg \min_{\forall \boldsymbol{s}_N \in \{\pm 1 \pm i\}^N} \left(\hat{\boldsymbol{S}}_N^{\mathrm{T}} \cdot \boldsymbol{Q} \cdot \hat{\boldsymbol{S}}_N\right) \tag{11}$$

where $\hat{\boldsymbol{S}}_N = [\hat{\boldsymbol{s}}_{N1}, \hat{\boldsymbol{s}}_{N2}, \ldots, \hat{\boldsymbol{s}}_{NM}]$, $\hat{\boldsymbol{s}}_{Ni} \in \mathbf{R}^N$, $i = 1, \ldots, M$ represents the ith estimated user sequence of length N. For the blind identification problem where the multi-users use the same frequency at the same time, because of the direct signal interference of the multi-users at the receiving end, it is impossible to directly use Hopfield neural network to solve (11) for multiple users. Therefore, the SSC method is used to separate the conventional user signals and the M2M communication users signals one by one from the received signal.

2. Conventional user signal detection

1) Performance function of conventional user signal's blind detection problem

Refer to the idea in references [15], [16], we introduce signal space cancellation (SSC) to restore conventional user signals. First, we estimate the conventional user signals $\hat{\boldsymbol{S}}_{N0}$ according to the following formula:

$$\hat{\boldsymbol{S}}_{N0} = \arg \min_{\forall \boldsymbol{s}_{N0} \in \{\pm 1 \pm i\}^N} \left(\hat{\boldsymbol{S}}_{N0}^{\mathrm{T}} \cdot \boldsymbol{Q} \cdot \hat{\boldsymbol{S}}_{N0}\right) \tag{12}$$

where $\boldsymbol{Q} = \boldsymbol{U}_N \boldsymbol{U}_N^{\mathrm{T}}$ meets the condition $\boldsymbol{Q}\hat{\boldsymbol{S}}_{N0} = 0$, and $\boldsymbol{U}_N$ is the unitary matrix in the singular value decomposition $\boldsymbol{y}_N = [\boldsymbol{U}, \boldsymbol{U}_N] \cdot \begin{bmatrix} \boldsymbol{D} \\ \boldsymbol{0} \end{bmatrix} \cdot \boldsymbol{V}^{\mathrm{T}}$ of the received signal matrix $\boldsymbol{y}_N$. We will use the CSHNN to solve the minimum value of (12).

2) The construction of complex Hopfield neural network

The network structure diagram of CSHNN as depicted in Fig.2.

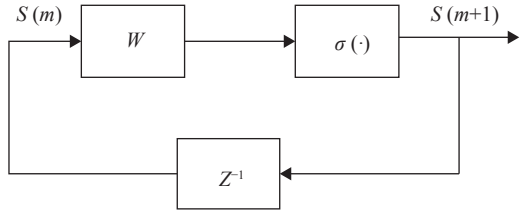

Fig. 2. The network structure diagram of CSHNN.

According to the above CSHNN network, we can list the state equation and output equation correspondingly. The state equation is

$$\begin{aligned} \boldsymbol{s}(m+1) &= \boldsymbol{s}_{\mathrm{R}}(m+1) + \mathrm{i}\boldsymbol{s}_{\mathrm{I}}(m+1) \\ &= \sigma_{\mathrm{R}}\left(\mathrm{Re}\left(\boldsymbol{W}\boldsymbol{s}(m)\right)\right) + \mathrm{i}\sigma_{\mathrm{I}}\left(\mathrm{Im}\left(\boldsymbol{W}\boldsymbol{s}(m)\right)\right) \\ &= \sigma\left(\boldsymbol{W}\boldsymbol{s}(m)\right) \end{aligned} \tag{13}$$

and the output equation is

$$\boldsymbol{y}(m) = \boldsymbol{W}\boldsymbol{s}(m) \tag{14}$$

where $\boldsymbol{s}(m)$ is the transmission signal of each neural network; $\boldsymbol{s} = [s_1, s_2, \ldots, s_N]$ is the send vector for neural network; $\boldsymbol{W}$ is the connection weight of each neuron, $\boldsymbol{W} \in \mathbf{C}^{N \times N}$ and $\boldsymbol{W}^{\mathrm{T}} = \boldsymbol{W}$; $\sigma(\cdot)$ is the activation function of the complex neural network. When the neural network reaches the final balance, it can be approximated as $\boldsymbol{y}(m) = \boldsymbol{s}(m)$, the obtained solution point signal $\boldsymbol{s}(m)$ is the signal sented by the conventional user to be detected.

In order to use HNN as a powerful tool to solve the problem of blind detection of traditional user, the connection weight matrix of the neural network can be configured as

$$\boldsymbol{W} = \boldsymbol{I} - \boldsymbol{Q} \tag{15}$$

When the complex HNN reaches equilibrium, that is $\boldsymbol{s}(m) = \boldsymbol{s}(m+1)$, which satisfies the requirements of the cost function. So the neural network weight matrix as above configuration can put the quadrature phase shift keying (QPSK) signal blind detection problem into an HNN energy function of the minimum problem. According to the proof of network stability in [17], it can be obtained that the stable convergence point of HNN is the needed sending signal.

It pointed out that if the blind detection algorithm is to achieve the goal of having a strong anti-interference ability, it is necessary to select the appropriate activation function of the HNN in [18].

3) Select the activation function of the complex Hopfiled neural network

At present, in many literatures which use the HNN to solve the blind detection problem, most of the activation functions use the sigmoid function [19], [20]. In information science, the sigmoid function is often used as the threshold function of neural networks due to its single increase and inverse function single increase. In order to adapt to complex channel and complex constellation signal QPSK, this paper refers to [21], [22] and compares the following five activation modes through simulation experiments, and selects the appropriate activation function.

$$\sigma_{\mathrm{R}}(x) = \sigma_{\mathrm{I}}(x) = \tanh(x) \tag{16}$$

$$\begin{aligned} \sigma_{\mathrm{R}}(x) &= \sigma_{\mathrm{I}}(x) \\ &= A\frac{\arctan(Bx_0) + 0.5\left(1 + \arctan(Bx - x_0)\right)}{1 + \arctan(Bx_0)}\varepsilon(x) \\ &\quad + A\frac{0.5\left(1 + \arctan(Bx - x_0)\right)}{1 + \arctan(Bx_0)}\varepsilon(-x) \end{aligned} \tag{17}$$

$$\sigma_{\mathrm{R}}(x) = \sigma_{\mathrm{I}}(x) = k\left(-1 + \left(2/\left(1 + e^{-\delta x}\right)\right)\right) \tag{18}$$

$$\sigma_{\mathrm{R}}(x) \ = \sigma_{\mathrm{I}}(x) \ = \arctan(x) \tag{19}$$

$$\sigma_{\mathrm{R}}(x) = \sigma_{\mathrm{I}}(x) = \mathrm{sign}(x) \tag{20}$$

where $A = 1$, $B = 50$, $k = 1$, $\delta = 0.5$; $\sigma_{\mathrm{R}}(x)$ and $\sigma_{\mathrm{I}}(x)$ denote the real part and the imaginary part of the sigmoid activation function.

The curves of the above five sigmoid activation functions named as tanh, new-atan, e, atan, and sign respectively, are shown in Fig.3. From Fig.3, it can be seen that:

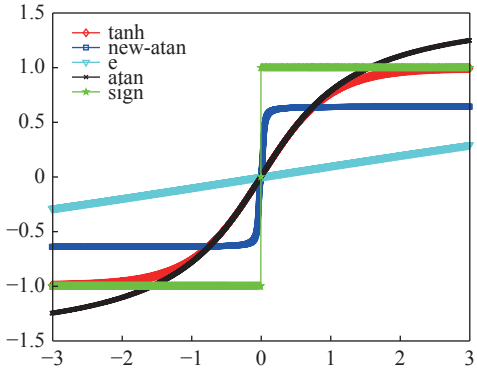

Fig. 3. Different sigmoid activation function.

i) The new-atan activation function and the sign rounded sigmoid activation function can ensure rapid convergence when the absolute value of the neuron input is large;

ii) Near the 0 point, the exponential activation function derivative value is smaller than the other four activation function derivative values, that is, the exp activation function is significantly less sensitive to the neuron input value near the 0 point.

Through experiments 1 and 2 in the Section V, the SSC-CSHNN network blind detection algorithm composed of the above five sigmoid functions is simulated and compared, and new-atan activation function is selected as the activation function of the SSC-CSHNN algorithm HNN.

The energy function of the SSC-CSHNN blind detection algorithm is expressed as

$$E(m) = -\frac{1}{2}\boldsymbol{s}(m)^{\mathrm{T}}\boldsymbol{W}\boldsymbol{s}(m) + \sum_{i=1}^{N}\left(\int_0^{\boldsymbol{s}_{\mathrm{R}i}(m)}\sigma^{-1}(x)\mathrm{d}x + \int_0^{\boldsymbol{s}_{\mathrm{I}i}(m)}\sigma^{-1}(x)\mathrm{d}x\right) \tag{21}$$

where E is the energy function of the network, the energy function is a variable related to the iteration time, the weight $\boldsymbol{W}$ moment satisfies $\boldsymbol{W} = \boldsymbol{W}^{\mathrm{T}}$, $\boldsymbol{s}(m)$ is the output of the neuron, and $\sigma^{-1}(x)$ is the inverse function of the sigmoid function $\sigma(x)$ of the neuron. According to the proof of the stability of the energy function in [23], [24], the energy function of the network is designed by referring to the network structure, and then the second theorem of Lyapunov can be used to prove the stability of the neural network.

3. Detect M2M communication signal by the signal space cancellation

It can be seen from Section III.2 that the transmission sequence $\hat{\boldsymbol{S}}_{N0}$ is the conventional user signals is restored, which is interference for M2M communication.

In order to restore the M2M communication signal, the restored conventional user signal is added to the noise space, and then a new complementary projection operator is reconstructed, and a new quadratic normalization algorithm is formed again to solve the problem, so as to obtain the signal sequence of the M2M communication.

The new secondary planning problem is

$$\hat{\boldsymbol{S}}_{Ni} = \arg \min_{\forall \boldsymbol{s}_{Ni} \in \{\pm 1 \pm i\}^N} \left(\hat{\boldsymbol{S}}_{Ni}^{\mathrm{T}} \cdot \boldsymbol{Q}' \cdot \hat{\boldsymbol{S}}_{Ni}\right) \tag{22}$$

The specific process is as follows. Suppose the first M2M device communication signal sequence is estimated using SSC, then $i = 1$. We add the calculated conventional user signal $\hat{\boldsymbol{S}}_{N0}$ to the complementary space of $\boldsymbol{y}_N$, and the signal space will be reduced to

$$\boldsymbol{U}_N' = \left[(\boldsymbol{U}_N)_{N\times(N-(L+1)P)} \vdots \hat{\boldsymbol{S}}_{N0}\right] \tag{23}$$

where $\hat{\boldsymbol{S}}_{N0}$ is the restored conventional user signal.

Perform singular value decomposition on (23), i.e.,

$$[\boldsymbol{U}_m, \boldsymbol{\Sigma}_m, \boldsymbol{V}_m] = SVD\,(\boldsymbol{U}_N') \tag{24}$$

where $\boldsymbol{U}_m = [\boldsymbol{U}_{1m} \vdots \boldsymbol{U}_{1n}]$, $\boldsymbol{U}_{1m}$ is the orthogonal basis of $\boldsymbol{U}_N'$.

The new complement space is thus obtained as

$$\boldsymbol{U}_{mN} = (\boldsymbol{U}_{1m})_{N\times(N-(L+1)P+M+1)} \tag{25}$$

Reconstruct the complementary projection operator $\boldsymbol{Q}' = \boldsymbol{U}_{mN} \cdot \boldsymbol{U}_{mN}^{\mathrm{T}}$, and substitute (22) to recover the M2M communication signal by using the same SSC-CSHNN blind detection algorithm as in the previous section. At this time, the estimated signal sequence of the first M2M device must not converge to the conventional user signal, so that the signal sequence of the first M2M device is restored. By analogy, the communication signal sequence of M2M devices ($i = 2, \ldots, M$) can be obtained one by one.

IV. Double Sigmoid Neural Network Blind Detection System

Since HNN has a delay limitation, the convergence

speed of the HNN energy function is an important factor considered in real-time applications. The conventional HNN cannot guarantee to obtain the global optimum, and often falls into the local optimum, and once it falls into the local optimum, the HNN needs to find the initial point again. Therefore, under the same optimization conditions, improving the convergence speed of the HNN is a necessary research point.

This section introduces the ideas of [22], [23], adding a sigmoid function to each neuron of the neural network, so that all neurons form a new double-sigmoid complex HNN, which is the neural network of the DSCHNN blind detection algorithm. The network structure diagram is shown in Fig.4.

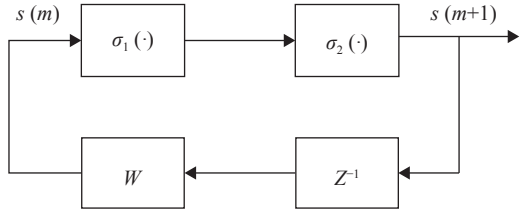

Fig. 4. Block diagram of blind detection algorithm based on SSC-DSCSHNN.

In Fig.4, $\boldsymbol{s}(m)$ is the transmission signal of each neural network; $\boldsymbol{W}$ is the weight matrix of the neuron, satisfying $\boldsymbol{W} \in \mathbf{C}^{N\times N}$, $\boldsymbol{W}^{\mathrm{T}} = \boldsymbol{W}$; $\sigma_1(\cdot)$, $\sigma_2(\cdot)$ are the two sigmoid functions of the neural network. When the neural network reaches equilibrium, that is $\boldsymbol{s}_0(m) = \boldsymbol{s}_0(m+1)$, the solution point signal obtained is the conventional user signal that needs to be detected.

For QPSK transmission signals, the state equation and the output equation of the blind detection algorithm SSC-DSCSHNN in this scheme are

$$\begin{aligned}\boldsymbol{s}(m+1) =& \boldsymbol{s}_{\mathrm{R}}(m+1) + \mathrm{i}\boldsymbol{s}_{\mathrm{I}}(m+1)\\ =& \sigma_{2\mathrm{R}}(\sigma_{1\mathrm{R}}(\mathrm{Re}(\boldsymbol{W}\boldsymbol{s}(m))))\\ &+ \mathrm{i}\sigma_{2\mathrm{I}}(\sigma_{1\mathrm{I}}(\mathrm{Im}(\boldsymbol{W}\boldsymbol{s}(m))))\\ =& \sigma_2(\sigma_1(\boldsymbol{W}\boldsymbol{s}(m)))\end{aligned} \tag{26}$$

$$\boldsymbol{y}(m) = \boldsymbol{W}\boldsymbol{s}(m) \tag{27}$$

where $\boldsymbol{s} = [s_1, s_2, \ldots, s_N]$ is the transmission vector of the neural network; $\boldsymbol{W}$ is the connection weight moment of each neuron, and $\boldsymbol{W} \in \mathbf{C}^{N\times N}$, $\boldsymbol{W}^{\mathrm{T}} = \boldsymbol{W}$; $\sigma_1(\cdot)$, $\sigma_2(\cdot)$ are the two sigmoid functions.

According to the selection analysis of the activation function in Section III.2.3) and related experimental simulations, this paper selects the sigmoid activation function (17) as the first activation function of the DSCHNN network.

In order to deeply analyze the impact of the double sigmoid structure on the performance of the blind detection network [22], [23], in this paper, we use the three formulas (18), (19), and (20) as the second sigmoid function of the DSCSHNN blind detection algorithm, in which $\delta, k > 0$. Hence, there are three double sigmoid functions used in this work, shortly named as new-atan+e, new-atan+atan, new-atan+sign respectively. In Section V, the performance of the SSC-DSCSHNN network formed by the three double sigmoid functions is simulated, the bit error rate and distance norm of the three are compared in detail, and the best combination is selected to form the SSC-DSCSHNN network and act as the double sigmoid activation function of this paper.

According to the idea of [18], suppose $\Delta E(m) = E(m+1) - E(m)$, only one neuron's state is updated in each feedback vector. Without losing generality, it is assumed that $s_n(m)$ is updated, then $\Delta s_n = s_n(m+1) - s_n(m) \neq 0$, $\Delta s_j = s_j(m+1) - s_j(m) = 0$, $j \neq n$.

$$\begin{aligned}\Delta E(m) &= E(m+1) - E(m)\\ &= -\frac{1}{2}\boldsymbol{s}^{\mathrm{T}}(m+1)\boldsymbol{W}\boldsymbol{s}(m+1) + \frac{1}{2}\boldsymbol{s}^{\mathrm{T}}(m)\boldsymbol{W}\boldsymbol{s}(m)\\ &\quad + \sum_{j=1}^{N}\int_{s_j(m)}^{s_j(m+1)} f^{-1}(x)\mathrm{d}x\\ &= -\frac{1}{2}\Delta\boldsymbol{s}^{\mathrm{T}}(m)\boldsymbol{W}\Delta\boldsymbol{s}(m) - \Delta\boldsymbol{s}^{\mathrm{T}}(m)\boldsymbol{W}\boldsymbol{s}(m)\\ &\quad + \sum_{j=1}^{N}\int_{s_j(m)}^{s_j(m+1)} f^{-1}(x)\mathrm{d}x\\ &= -\frac{1}{2}\Delta s_n^2 w_{nn} - \Delta s_n \cdot f^{-1}(s_n(m+1))\\ &\quad + \int_{s_n(m)}^{s_n(m)+\Delta s_n} f^{-1}(x)\mathrm{d}x\\ &= -\frac{1}{2}\Delta s_n^2 w_{nn} - \Delta s_n \cdot f^{-1}(s_n(m+1))\\ &\quad + \Delta s_n \cdot f^{-1}(s_n(m+1)) - \frac{1}{2}(\Delta s_n)^2\left[f^{-1}(\xi_n)\right]'\\ &= -\frac{1}{2}\Delta s_n^2\left\{w_{nn} + \left[f^{-1}(\xi_n)\right]'\right\}\end{aligned}$$

where $\Delta\boldsymbol{s}(m) = \boldsymbol{s}(m+1) - \boldsymbol{s}(m)$, $f^{-1}(\cdot)$ is the inverse function of activation function $f(\cdot)$. The fifth equation is based on Taylor's theorem.

$$\begin{aligned}\int_{s_n(m)}^{s_n(m+1)} f^{-1}(x)dx =& \Delta s_n \cdot f^{-1}(s_n(m+1))\\ &- \frac{1}{2}(\Delta s_n)^2\left[f^{-1}(\xi_n)\right]'\end{aligned} \tag{28}$$

where ξ_n satisfies $s_n(m) \le \xi_n \le s_n(m+1)$ or $s_n(m+1) \le \xi_n \le s_n(m)$.

Assume that $\mu = \min\left\{\left[f^{-1}(\xi_j)\right]' | j = 1, \ldots, N\right\}$, because $f^{-1}(\cdot)$ increases monotonically, there must be $\mu > 0$.

To sum up, as long as $[w_{nn}+\mu]>0$, $\forall n$, the inequality $\Delta E(m)<0$ can be guaranteed. Only if $\boldsymbol{s}(m)=\boldsymbol{s}(m+1)$, $\Delta E(m)=0$ can be guaranteed, the network reaches equilibrium. It shows that the energy of the network gradually decreases during operation, and finally converges to a stable equilibrium state.

The energy function of the SSC-DSCSHNN blind detection algorithm in this paper is expressed as

$$E(m)=-\frac{1}{2}\boldsymbol{s}(m)^{\mathrm{T}}\boldsymbol{W}\boldsymbol{s}(m)+\sum_{i=1}^{N}\left(\int_{0}^{\boldsymbol{s}_{Ri}(m)}\sigma_i^{-1}(x)\mathrm{d}x+\int_{0}^{\boldsymbol{s}_{Ii}(m)}\sigma_i^{-1}(x)\mathrm{d}x\right) \tag{29}$$

where E is the energy function of the network, the energy function is a variable related to the iteration time, the weight $\boldsymbol{W}$ moment satisfies $\boldsymbol{W}=\boldsymbol{W}^{\mathrm{T}}$, $\boldsymbol{s}(m)$ is the output of the neuron, and $\sigma_i{}^{-1}(x)$ is the inverse function of $\sigma_i(x)$, i represents the ith sigmoid function. According to reference [25], it can be concluded that SSC-DSCSHNN network is a stable structure. The value of the energy function of SSC-DSCSHNN becomes less and less in the iterative process, and the final system is in a stable state of convergence.

V. Simulations

M2M communication plays an important role in many fields, among which people's demand for smart grid is a powerful driving force for the development of M2M communication [26]. Phasor measurement unit (PMU), as the main equipment of the smart grid, can be used in the fields of dynamic monitoring, system protection, system analysis and prediction of the power system, and is an important equipment to ensure the safe operation of the power grid [27]. Therefore, the M2M communication in this paper is completed by simulating the PMU communication in the smart grid. This text combines the user datagram protocol (UDP) packet and PMU sampling data to form M2M transmission signal. Each group of sampled data consists of the following sampled values: time, voltage amplitude, voltage angle, voltage frequency and current of adjacent lines. We use 16-bit A/D to quantize the data and convert the bit sequence into a QPSK symbol sequence.

Simulation environment Conventional users and M2M sending signals are QPSK signals, and the noise is additive white Gaussian noise. The simulation results are obtained after 100 Monte Carlo experiments. Set the point where the bit error rate is zero to facilitate comparison with the CSHNN algorithm.

1) Experiment 1: Comparison of bit error rate and convergence time

Fixed QPSK transmission signal data length as $N=80$, using random channels with varying weights and delays. Under this condition, when comparing the following five different sigmoid functions as the activation function of the SSC-CSHNN neural network, the bit error rate of the conventional user signal and the M2M communication signal and the algorithm convergence time are compared. Sigmoid activation functions are: tanh, new-atan, e, atan, sign.

It can be seen from Table 1 that the corresponding algorithms of e activation function and new-atan activation function run slowly, but within the acceptable range, the corresponding algorithms of the other three activation functions run shorter.

Table 1. Operation time of five activation function algorithms

Activation function	tanh	new-atan	e	atan	sign
Operation time (s)	86.741	175.562	137.626	110.476	41.9499

It can be seen from Fig.5 that when the signal-to-noise ratio is 10 dB, except for the exp index and the tanh activation function, the error rate of the neural network composed of the other three activation functions all drops to 0. It can be seen from Fig.6 that for sparse QPSK signals, the tanh activation function has a bit error rate of 0 when the minimum signal-to-noise ratio is 18 dB, and the new-atan activation function and the sign rounding activation function reach the bit error rate when the signal-to-noise ratio is 24 dB. Zero point, the error rate of the other two activation functions is always higher than other algorithms before it drops to zero. Comprehensively available: tanh activation function shows good performance in terms of bit error rate, anti-noise ability or time complexity, but it is sensitive to neuron input; the network composed of new-atan activation function has strong anti-noise ability, but the corresponding time complexity is relatively

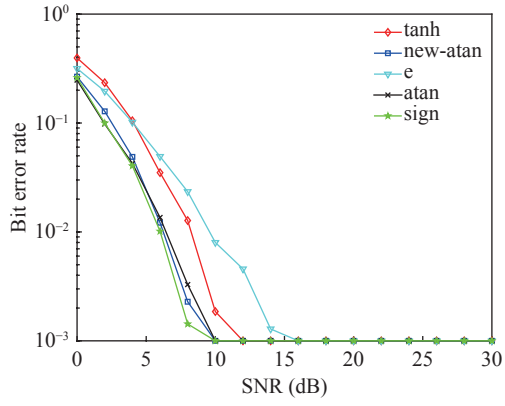

Fig. 5. Comparison of conventional user bit error rate under different Sigmoid activation functions.

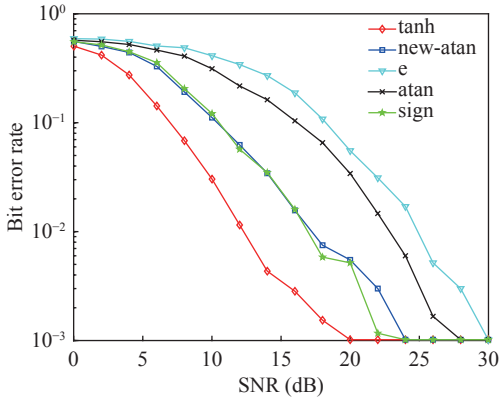

Fig. 6. Comparison of M2M communication bit error rate under different sigmoid activation functions.

high.

2) Experiment 2: Convergence speed comparison

In the case of a signal-to-noise ratio of 10 dB, the fixed QPSK transmission signal data length is $N = 80$, using a random synthesis channel with varying delays and varying weights. The SSC-CSHNN blind detection algorithm is simulated under five different activation functions, including tanh, new-atan, exp index, atan and sign. In this experiment, the number of iterations is used to reflect the convergence speed of the algorithm, and the distance norm L_2 is used to reflect the performance index of this experiment. The distance norms of the above five activation function algorithms are shown in Fig.7.

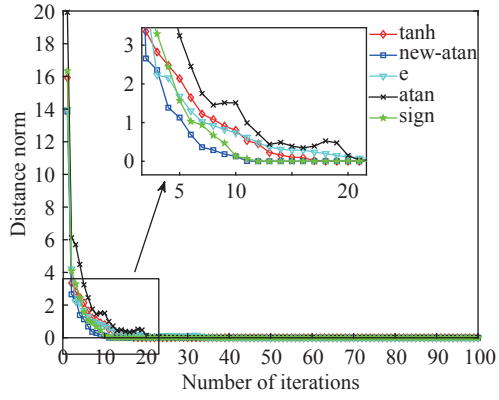

Fig. 7. Comparison of distance norms of five activation function algorithms.

The norm of a vector refers to the length of the quantity. Its mathematical definition is: the norm $\| x \|$ of a vector must satisfy $\| x \| \geq 0$, $\| cx \| = |c| \cdot \| x \|$ and $\| x + y \| \leq \| x \| + \| y \|$. The norm L_2 of text selection $(L_2 = \left(\sum_{i=0}^{n} \| x_i \|^2\right)^{\frac{1}{2}})$.

The zero point of the distance norm is the network equilibrium point. From Fig.7 and Table 2, it can be seen that the algorithm composed of the new-atan activation function decreases to 0 when the number of iterations is 11; and the algorithm composed of the sign activation function decreases the value of the distance norm when the number of iterations is 12. When it drops to 0, the distance norm of the algorithm composed of tanh activation function drops to 0 when the number of iterations is 18, while the algorithm composed of exp exponential activation function and atan needs more than 20 iterations to reduce the distance norm to 0. In the simulation, when the value of the distance norm drops to 0, the network reaches an equilibrium state. It can be seen that: under the same initial test conditions, among the algorithms composed of five activation functions, the algorithm composed of new-atan activation functions has the fastest convergence speed. Synthesizing experiment 1 and experiment 2, it can be concluded that the new-atan activation function algorithm has the fastest convergence speed, better error performance and anti-noise performance, so the sigmoid activation function of the SSC-CSHNN neural network selects the new-atan activation function.

Table 2. Neural network iteration times under five activation functions

Activation function	tanh	new-atan	exp	atan	sign
Number of iterations	18	11	20+	20+	12

3) Experiment 3: Comparison of SSC-CSHNN algorithm bit error rate under different channels

The fixed QPK signal transmission sequence data length is $N = 80$, and the SSC-CSHNN blind detection algorithm is simulated under the following five different channel conditions. CH1: a composite channel with fixed weights and delays and no common zero; CH2: a composite channel with fixed weights and delays, and a composite channel with a common zero; CH3: fixed weights and delays, A composite channel with two common zeros; CH4: a random composite channel with varying weights and delays; CH5: The channel of [12] with delay $= [0, 1/3]$ and weight coefficient $= [1, -0.7]$, which adds zeros at the beginning and end of the channel. Under the above five different channel conditions, the SSC-CSHNN blind detection algorithm is used to recover the bit error rate of conventional user signals and M2M communication signals as shown in Figs.8 and 9.

In conventional user signal detection, under the random synthetic channel CH4 with varying weights and delays, the bit error rate (BER) of the SSC-CSHNN algorithm is reduced to 0 when the signal-to-noise ratio (SNR) is 12 dB; in the synthetic channel without common zeros when the signal-to-noise ratio of CH1 is 14 dB, it drops to 0; the composite channel CH2 with one common zero is reduced to 0 when the signal-to-noise

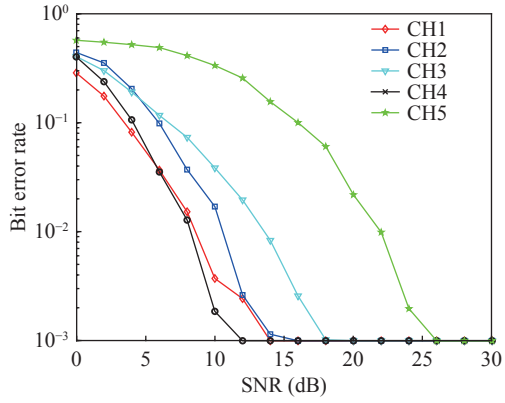

Fig. 8. The SSC-CSHNN blind detection algorithm restores the bit error rate of conventional user signals.

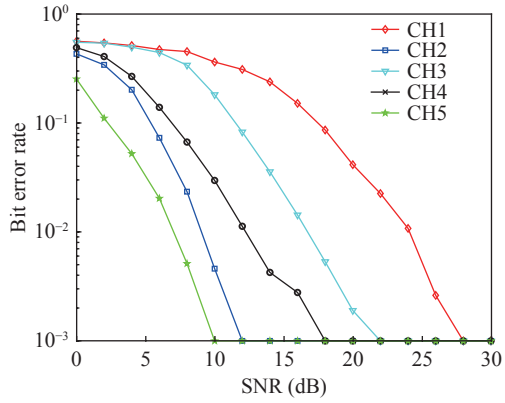

Fig. 9. SSC-CSHNN blind detection algorithm to recover M2M communication signal error rate.

ratio is 16 dB; the composite channel CH3 with two common zeros is reduced to 0 when the signal-to-noise ratio is 18 dB.; When the SNR of the channel of [12] CH5 is 26 dB, it will be reduced to 0.

In the detection of M2M communication signals, under the random synthetic channel CH4 with varying weights and delays, the bit error rate of the SSC-CSHNN algorithm is reduced to 0 when the signal-to-noise ratio is 18 dB; in the synthetic channel without common zeros, the signal-to-noise ratio under CH1 is reduced to 0 when it is 28 dB; the composite channel CH2 with one common zero is reduced to 0 when the signal-to-noise ratio is 12 dB; the composite channel CH3 with two common zeros is reduced to 0 when the signal-to-noise ratio is 22 dB; When the SNR of the channel of [12] CH5 is 10 dB, it will be reduced to 0.

It can be seen from Figs.8 and 9 that the SSC-CSHNN blind detection algorithm has certain applicability under different classical channels.

4) Experiment 4: Data length comparison

This experiment is carried out under the condition that the data length of the traditional transmission sequence and the data length of the M2M communication signal are both: 40, 60, 80, 100, 200, 300, 400, to compare the detection of the SSC-CSHNN blind detection algorithm proposed in this article The relationship between the bit error rate of traditional user signals and M2M communication signals and the length of the transmitted data is shown in Figs.10 and 11. Among them, the transmission channel is a composite channel with fixed weights and delays and without common zeros. Under the condition of 30 dB signal-to-noise ratio at the same time, when the M2M signal transmission sequence data length is 40, 50, 60, the constellation diagram of the signal before the 100th Monte Carlo experiment and the signal has not passed the sigmoid activation function is shown in Fig.12.

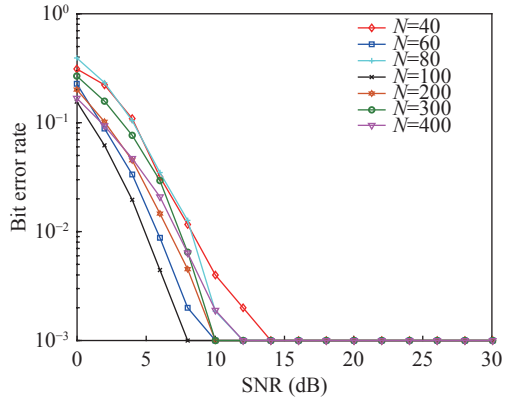

Fig. 10. Comparison of bit error rate under different traditional user data volume of SSC-CSHNN algorithm.

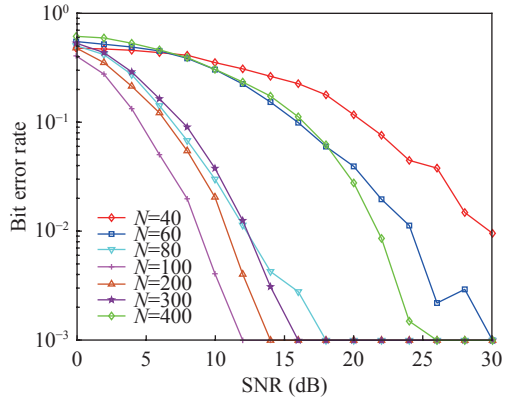

Fig. 11. Comparison of bit error rate under different M2M signal data volume of SSC-CSHNN algorithm.

The SSC-CSHNN algorithm proposed in this article requires a data length greater than or equal to 60 to obtain stable M2M signal detection results, and the data length is increased from 40 to 100 at a scale ratio of 20, and the algorithm's anti-interference ability and error code performance are getting better and better. The data length is increased from 100 to 400 with 100 arithmetic, the algorithm's anti-interference ability and error code performance are reduced, but the mixed sig-

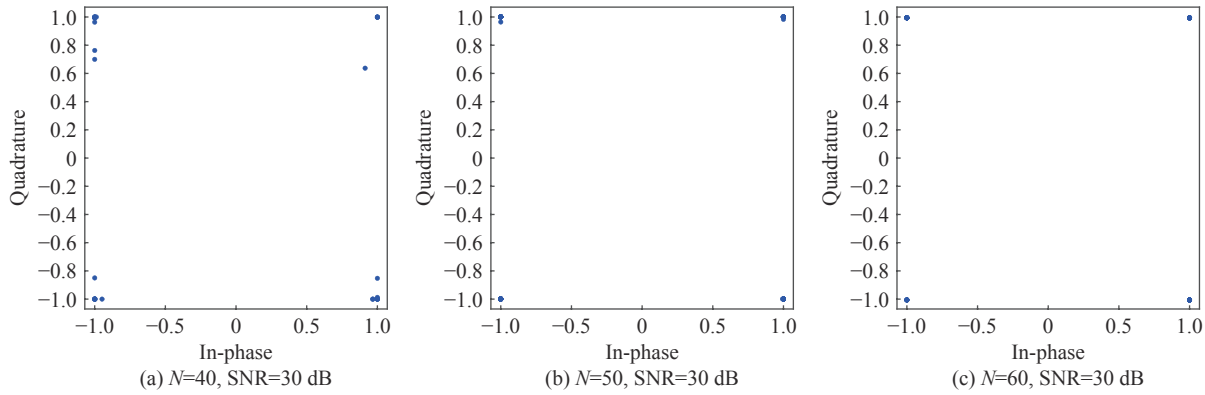

Fig. 12. The constellation diagram of the M2M communication signal under different data lengths for the SSC-CSHNN algorithm.

nal can still be recovered well.

Comparing the three constellation diagrams in Fig.12, it can be seen that the distribution of points at $N = 40$ is relatively scattered, and the positions of the four groups of points can be clearly distinguished; the distribution of points at $N = 50$ tends to be compact; the distribution of points at $N = 60$ is more compact, which shows that the neuron state of the SSC-CSHNN algorithm finally converges to the four equilibrium points, and it becomes easier to converge when the length of the input data increases. The experimental results show that the SSC-CSHNN blind detection algorithm proposed in this section requires a shorter amount of data. The larger the data length, the better the performance of the algorithm. The SSC-CSHNN algorithm has better applicability in a relatively short data volume environment.

5) Experiment 5: Comparison of bit error rate

Fixed QPSK transmission signal data length $N = 80$, using random channels with varying weights and delays. Under this condition, compare the bit error rates of traditional user signals and M2M communication signals when the three different dual sigmoid functions described in Section III.2.2) are used as the activation function of the SSC-DSCSHNN neural network. And give the bit error rate comparison chart when the fixed signal-to-noise ratio is 8 dB. The simulation results are shown in Figs.13–15.

It can be seen from Fig.13 that the double sigmoid activation function neural network composed of new-atan and sign and atan respectively has a bit error rate of 0 when the signal-to-noise ratio is 8 dB, while the neural network composed of new-atan and exp is in the signal-to-noise ratio. When it is 12 dB, the zero bit error rate is reached. It shows that for traditional user signals, the former has better anti-interference ability than the latter.

It can be seen from Fig.14 that the double sigmoid activation function neural network composed of new-atan and e and atan respectively has a bit error rate of

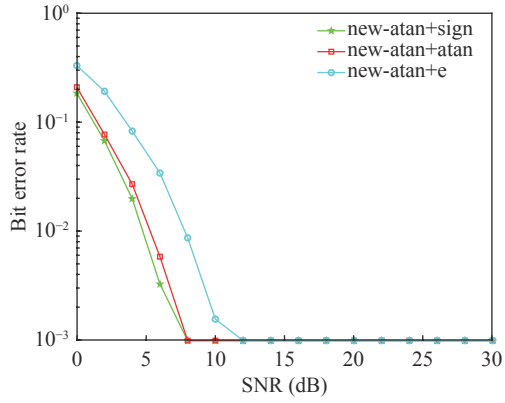

Fig. 13. Comparison of traditional user bit error rate under different dual sigmoid function algorithms.

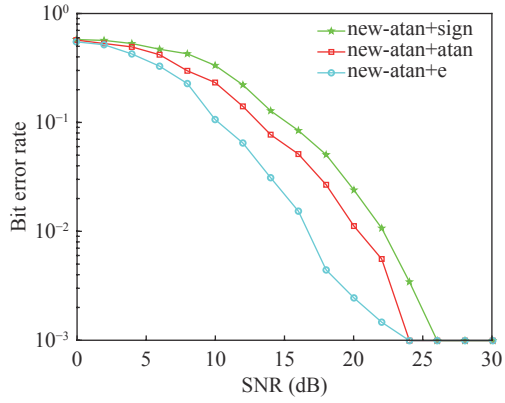

Fig. 14. Comparison of M2M communication signal bit error rate under different dual sigmoid function algorithms.

0 when the signal-to-noise ratio is 24 dB, while the neural network composed of new-atan and sign is in the signal-to-noise ratio When it is 26 dB, the bit error rate zero point is reached. It shows that for sparse M2M communication signals, the former has better anti-interference ability than the latter.

6) Experiment 6: Convergence speed comparison

In the case of a signal-to-noise ratio of 10 dB, the fixed QPSK transmission signal data length is N =80,

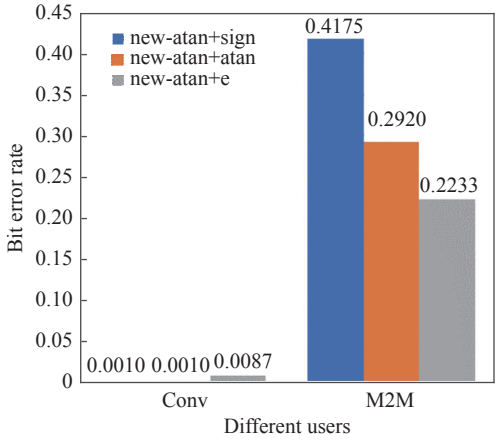

Fig. 15. The bit error rate of the algorithm under different dual sigmoid functions at 8 dB.

using a random synthesis channel with varying delays and varying weights, and combining three different Sigmoid activation functions into the SSC-DSCSHNN detection algorithm for simulation. In the experiment, the distance norm is used as the performance index to compare the convergence speed of the algorithm as shown in Fig.16.

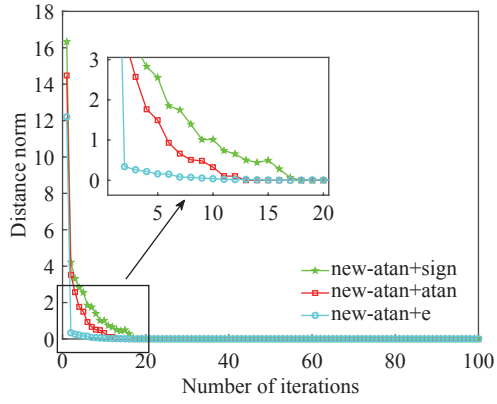

Fig. 16. Comparison of distance norms under three dual sigmoid activation function algorithms.

It can be seen from Fig.16 that the double sigmoid activation function algorithm formed by new-atan+e decreases the value of the distance norm to 0 when the number of iterations is 10, and the value of the distance norm drops to 0 when the number of iterations of the other algorithms is 13 and 17. When the value of the distance norm drops to 0 in the simulation, the network reaches a balanced state. It can be seen from the figure that under the same initial test conditions, among the three double sigmoid activation functions, the SSC-CSHNN algorithm formed by the new-atan and exp activation functions has the fastest convergence speed.

Combining experiment 5 and experiment 6, it can be concluded that the SSC-DSCSHNN algorithm composed of new-atan and exp activation functions has the fastest convergence speed, better error performance and noise resistance. Therefore, the dual sigmoid activation function selects new-atan and exp activation function.

7) Experiment 7: Comparison of bit error rate and convergence speed

The transmission sequence data length of a fixed signal is $N = 80$, and a random channel with varying weights and delays is used. Compare the bit error rate of CSHNN algorithm, SSC-CSHNN algorithm and SSC-DSCSHNN algorithm in [7], as shown in Fig.17.

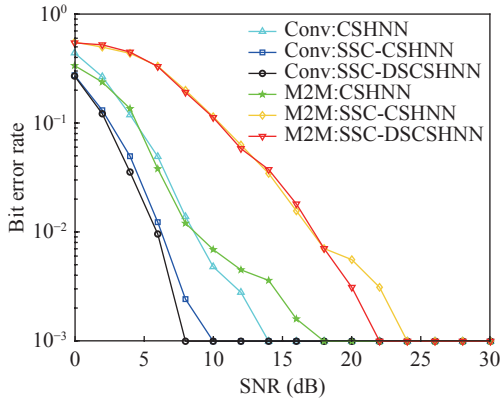

Fig. 17. Comparison of the bit error rate of CSHNN, SSC-CSHNN and SSC-CSHNN algorithms.

The activation function is the core of the neural network. It can be seen from Fig.17 that for traditional user signals, under the same initial conditions, the SSC-CSHNN algorithm achieves zero bit error rate at the lowest signal-to-noise ratio (8 dB), the traditional activation function SSC-CSHNN algorithm and the improved activation function SSC-CSHNN. the bit error rate of the algorithm is reduced to 0 at 10 dB and 12 dB respectively. Therefore, the introduction of the dual sigmoid function further improves the anti-interference ability of the network.

When the signal-to-noise ratio is 10 dB, the CSHNN algorithm, SSC-CSHNN algorithm, and SSC-DSCSHNN algorithm of [7] are used to compare the number of iterations when the value of the distance norm drops to 0, as shown in Table 3.

Table 3. Number of iterations of the three algorithms

Algorithm	CSHNN	SSC-CSHNN	SSC-DSCSHNN
Number of iteration	18	11	10

It can be seen from Table 3 that the SSC-DSCSHNN algorithm further improves the convergence speed of the algorithm, making the neural network obtain better performance.

8) Experiment 8: Comparison of bit error rate and convergence speed

Fixed QPSK transmission signal data length $N = 80$, using random channels with varying weights and delays. Compare the bit error rate of several classical algorithms, SSC-CSHNN algorithm, SSC-CSHNN algorithm with improved activation function and SSC-DCSHNN algorithm composed of new-atan and e proposed in this paper, as shown in Fig.18. The operation time comparison of different algorithms under fixed signal-to-noise ratio of 12 dB and 24 dB is shown in Fig.19.

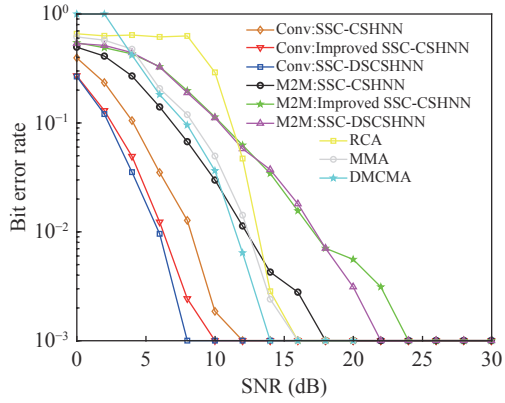

Fig. 18. Comparison of the bit error rate of several classical algorithms, SSC-CSHNN, Improved SSC-CSHNN and SSC-DCSHNN algorithms.

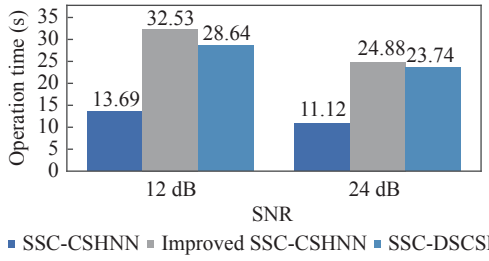

Fig. 19. Comparison of the operation time of SSC-CSHNN, improved SSC-CSHNN and SSC-DCSHNN algorithms.

Activation function is the core of neural network. It can be seen from Fig.18 that for traditional user signals, under the same initial conditions, the bit error rate of SSC-DSCSHNN algorithm reaches zero at the lowest signal-to-noise ratio (8 dB), and the bit error rate of SSC-CSHNN algorithm of classical activation function and SSC-CSHNN algorithm of improved activation function is reduced to 0 at 10 dB and 12 dB respectively. Therefore, the introduction of double sigmoid function further improves the anti-interference ability of the network. It can be seen from Fig.19 that the SSC-DSCSHNN algorithm runs faster than the SSC-CSHNN algorithm with improved activation function, but slower than the SSC-CSHNN algorithm with classical activation function, but within the acceptable range.

Combining Experiment 2 and Experiment 6, the comparison of the number of iterations of SSC-CSHNN algorithm using classical activation function, the SSC-CSHNN algorithm with improved activation function and SSC-DSCSHNN algorithm when the value of distance norm drops to 0 is given in Table 4 when the signal-to-noise ratio is 10 dB.

Table 4. Number of iterations of the three algorithms

Algorithm	SSC-CSHNN	Improved SSC-CSHNN	SSC-DSCSHNN
Number of iteration	18	11	10

It can be seen from Table 4 that when the distance norm of SSC-DSCSHNN algorithm decreases to 0, the number of iterations required by the neural network is the least, that is, the convergence speed is faster and the neural network performance is better.

Comprehensive Experiment 8 concludes that the SSC-DSCSHNN algorithm using double sigmoid function improves the anti-noise performance and convergence speed of SSC-CSHNN algorithm on the basis of ensuring time efficiency.

On the whole, it can be seen that SSC-DSCSHNN algorithm using dual sigmoid functions improves the anti-noise performance and convergence speed of the SSC-CSHNN algorithm on the basis of ensuring time efficiency.

VI. Conclusions

In this paper, in the M2M communication and conventional user communication spectrum sharing system, different activation functions are selected to improve the SSC-CSHNN blind detection algorithm. The disadvantages of poor anti-noise performance, slower convergence speed, and large neuron sensitivity to input are proved by simulation and comparison. The convergence speed of the blind detection algorithm of activation function has been improved to a certain extent. In order to further improve the network's anti-interference ability and convergence speed, this paper refers to the dual sigmoid idea, proposes the SSC-DSCSHNN blind detection algorithm, and compares and selects the dual sigmoid activation functions through simulation experiments such as bit error rate and distance norm, and finally compares the simulations. Error performance and convergence speed of SSC-CSHNN algorithm and SSC-DSCSHNN algorithm. The simulation results show that the signal space deletion method successfully separates the mixed signals of M2M and conventional users. The SSC-CSHNN algorithm improves the anti-noise performance of the network to a certain extent. The proposed complex Hopfield blind detection al-

gorithm is robust to different channels. A very short amount of data is required to obtain better error performance. Under the condition of the same signal-to-noise ratio, the simulation comparison with the distance norm between the state vector and the equilibrium point as the index shows that the SSC-DSCSHNN algorithm can significantly and effectively accelerate the convergence speed of the algorithm compared with the SSC-CSHNN algorithm, and greatly optimize the neural network. It can be seen that the solution proposed in this paper solves the problem of using the statistical characteristics of the receiving end signal to recover the transmitted signal when the channel is unknown. It is more in line with the characteristics of the actual transmission channel and avoids the channel overhead and the waste of spectrum resources caused by the use of training sequences.

References

[1] A. Ali, G. A. Shah, and J. Arshad, "Energy efficient techniques for M2M communication: A survey," *Journal of Network and Computer Applications*, vol.68, pp.42–55, 2016.

[2] Y. Mehmood, C. Görg, M. Muehleisen, *et al.*, "Mobile M2M communication architectures, upcoming challenges, applications, and future directions," *EURASIP Journal on Wireless Communications and Networking*, vol.2015, no.1, article no.250, 2015.

[3] P. K. Verma, R. Verma, A. Prakash, *et al.*, "Machine-to-machine (M2M) communications: A survey," *Journal of Network and Computer Applications*, vol.66, pp.83–105, 2016.

[4] H. Shariatmadari, R. Ratasuk, S. Iraji, *et al.*, "Machine-type communications: Current status and future perspectives toward 5G systems," *IEEE Communications Magazine*, vol.53, no.9, pp.10–17, 2015.

[5] A. Biral, M. Centenaro, A. Zanella, *et al.*, "The challenges of M2M massive access in wireless cellular networks," *Digital Communications and Networks*, vol.1, no.1, pp.1–19, 2015.

[6] A. S. Lioumpas and A. Alexiou, "Uplink scheduling for machine-to-machine communications in LTE-based cellular systems," in *Proceedings of 2011 IEEE GLOBECOM Workshops*, Houston, TX, USA, pp.353–357, 2011.

[7] T. Kim, K. S. Ko, and D. K. Sung, "Prioritized random access for machine-to-machine communications in OFDMA based systems," in *Proceedings of 2015 IEEE International Conference on Communications*, London, UK, pp.2967–2972, 2015.

[8] X. H. Li, J. Zheng, and M. J. Zhang, "Compressive sensing based spectrum sharing and coexistence for machine-to-machine communications," in *Proceedings of 2017 IEEE International Conference on Acoustics, Speech and Signal Processing*, New Orleans, LA, USA, pp.3604–3608, 2017.

[9] A. T. Abebe and C. G. Kang, "Overlaying machine-to-machine (M2M) traffic over human-to-human (H2H) traffic in OFDMA system: Compressive-sensing approach," in *Proceedings of 2016 International Conference on Selected Topics in Mobile & Wireless Networking*, Cairo, Egypt, pp.1–6, 2016.

[10] J. Zhang, X. Wang, and X. J. Yang, "A method of constellation blind detection for spectrum efficiency enhancement," in *Proceedings of the 2016 18th International Conference on Advanced Communication Technology*, PyeongChang, Korea (South), pp.148–152, 2016.

[11] Z. F. Yuan, Y. Z. Hu, W. M. Li, *et al.*, "Blind multi-user detection for autonomous grant-free high-overloading multiple-access without reference signal," in *Proceedings of the 2018 IEEE 87th Vehicular Technology Conference*, Porto, Portugal, pp.1–7, 2018.

[12] Y. Zhang and Z. Y. Zhang, "Blind detection of 64QAM signals with a complex discrete Hopfield network," *Journal of Electronics & Information Technology*, vol.33, no.2, pp.315–320, 2011. (in Chinese)

[13] Q. Y. Quan, "A multilevel Hopfield neural network for OFDM system with phase noise," in *Proceedings of the 2009 7th International Conference on Information, Communications and Signal Processing*, Macau, China, pp.1–5, 2009.

[14] Y. Zhang, B. R. Li, S. J. Yu, *et al.*, "Blind detection algorithm based on spectrum sharing and coexistence for machine-to-machine communication," *IEICE TRANSACTIONS on Fundamentals of Electronics, Communications and Computer Sciences*, vol.E103.A, no.1, pp.297–302, 2020.

[15] R. Hu, "The study of blind processing system based on clustering virtual MIMO wireless sensor networks," *Master Thesis*, Nanjing University of Posts and Telecommunications, Nanjing, China, pp. 9 - 28 , 2015. (in Chinese)

[16] Z. Z. Zhang, "Blind detection system based on clustering virtual MIMO wireless sensor networks," *Master thesis*, Nanjing University of Posts and Telecommunications, Nanjing, China, pp. 12 -17 , 2014. (in Chinese)

[17] X. K. Ruan and Z. Y. Zhang, "Blind detection of QAM signals using continuous Hopfield-type neural network," *Journal of Electronics & Information Technology*, vol.33, no.7, pp.1600–1605, 2011. (in Chinese)

[18] D. Feng, S. J. Yu, and Y. Zhang, "Blind detection algorithm of Hopfield neural network with improved activation function," *Computer Technology and Development*, vol.22, no.12, pp.207–210, 2012. (in Chinese)

[19] M. A. Zaveri, S. N. Merchant, and U. B. Desai, "Robust neural-network-based data association and multiple model-based tracking of multiple point targets," *IEEE Transactions on Systems, Man, and Cybernetics, Part C (Applications and Reviews)*, vol.37, no.3, pp.337–351, 2007.

[20] S. J. Yu, D. Feng, and Y. Zhang, "Blind detection of BPSK signals using hysteretic Hopfield neural network," in *Proceedings of 2013 Chinese Intelligent Automation Conference: Intelligent Automation*, Z. Q. Sun and Z. D. Deng, Eds. Springer, Berlin, Germany, pp.693–701, 2013.

[21] S. W. Chen, S. J. Yu, Z. M. Zhang, *et al.*, "A novel blind detection algorithm based on adjustable parameters activation function Hopfield neural network," *Journal of Information Hiding and Multimedia Signal Processing*, vol.8, no.3, pp.670–675, 2017.

[22] Z. Uykan, "Fast-convergent double-sigmoid Hopfield neural

network as applied to optimization problems," *IEEE Transactions on Neural Networks and Learning Systems*, vol.24, no.6, pp.990–996, 2013.

[23] Y. Shen and J. Wang, "Robustness analysis of global exponential stability of recurrent neural networks in the presence of time delays and random disturbances," *IEEE Transactions on Neural Networks and Learning Systems*, vol.23, no.1, pp.87–96, 2012.

[24] A. Balavoine, J. Romberg, and C. J. Rozell, "Convergence and rate analysis of neural networks for sparse approximation," *IEEE Transactions on Neural Networks and Learning Systems*, vol.23, no.9, pp.1377–1389, 2012.

[25] J. Nong, "Global exponential stability of delayed Hopfield neural networks," in *Proceedings of 2012 International Conference on Computer Science and Information Processing*, Xi'an, China, pp.193–196, 2012.

[26] M. Emmanuel and R. Rayudu, "Communication technologies for smart grid applications: A survey," *Journal of Network and Computer Applications*, vol.74, pp.133–148, 2016.

[27] L. Zora, D. Elizondo, S. M. Jaramillo, *et al.*, "PMU applications prioritization methodology using wide-area disturbances events and its implementation in the Colombian electric power system," in *Proceedings of 2017 IEEE Power & Energy Society General Meeting*, Chicago, IL, USA, pp.1–5, 2017.

ZHANG Yun was born in Nanjing, Jiangshu Province, China, in 1977. She received the M.S. and Ph.D. degrees from Nanjing University of Posts and Telecommunication, Nanjing, China, in 2005 and 2011 respectively. She has been a lectorate with the college of Electrical Science and Engineering, Nanjing University of Posts and Telecommunication since 2012. Her research interests are in the fields of adaptive signal processing, blind channel equalization, and digital wireless communications. (Email: y021001@njupt.edu.cn)

ZHOU Jing was born in Changzhou, Jiangsu Province, China, in 1998. She is a master student of Nanjing University of Posts and Telecommunications. Her research directions are intelligent signal processing and communication signal processing.
(Email: Z_Jing1020@163.com)

LIU Rong was born in Nantong, Jiangsu Province, China, in 1999. He is a master student of Nanjing University of Posts and Telecommunications. His research directions are intelligent signal processing and communication signal processing.
(Email: 1021020927@njupt.edu.cn)

YU Shujuan was born in Hailar, Inner Mongolia, China, in 1967. She received the B.E. and M.S. degrees from Harbin Institute of Technology, Harbin, China, in 1989 and Southeast University, Nanjing, China, in 1995 respectively. She has been an Associate Professor and Master Tutor at College of Electronic and Optical Engineering, Nanjing University of Posts and Telecommunications since 2007.
(Email: yusj@njupt.edu.cn)

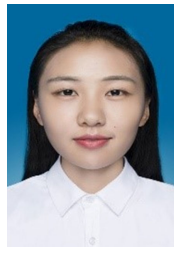

LI Binrui was born in Anyang, Henan Province, China, in 1997. She received the M.S. degree in Nanjing University of Posts and Telecommunications. Her research directions are intelligent signal processing, wireless sensor network, and communication signal processing.
(Email: 1419866124@njupt.edu.cn)